VENUS: MEASUREMENTS OF MICROWAVE BRIGHTNESS TEMPERATURES AND INTERPRETATIONS OF THE RADIO AND RADAR SPECTRA

BY

WILLIAM WALLACE WARNOCK

B.S., University of Illinois, 1967

THESIS

Submitted in partial fulfillment of the requirements
for the degree of Doctor of Philosophy in Astronomy
in the Graduate College of the
University of Illinois at Urbana-Champaign, 1971

Urbana, Illinois

UNIVERSITY OF ILLINOIS AT URBANA-CHAMPAIGN

THE GRADUATE COLLEGE

Observatory

September, 1971

I HEREBY RECOMMEND THAT THE THESIS PREPARED UNDER MY SUPERVISION BY William Wallace Warnock

ENTITLED VENUS: MEASUREMENTS OF MICROWAVE BRIGHTNESS TEMPERATURES AND INTERPRETATIONS OF THE RADIO AND RADAR SPECTRA

BE ACCEPTED IN PARTIAL FULFILLMENT OF THE REQUIREMENTS FOR THE DEGREE OF Doctor of Philosophy in Astronomy

G. W. Swenson Jr.
In Charge of Thesis

G. W. Swenson, Jr.
Head of Department

Recommendation concurred in†

Paul Handler
R. G. Langebartel
S. P. Wyatt, Jr.
John R. Dickel

Committee on Final Examination†

† Required for doctor's degree but not for master's.

D517

ACKNOWLEDGMENT

Foremost thanks are extended to my research adviser, Dr. John R. Dickel, who has continuously given me assistance and encouragement throughout my graduate studies. I also thank the other members of my Doctoral Committee, Drs. George W. Swenson, Jr., Stanley P. Wyatt, Jr., Ray G. Langebartel, and Paul Handler, for their advice and cooperation.

I appreciate the use of the facilities at the Algonquin Radio Observatory and the National Radio Astronomy Observatory. The directors and staffs of these observatories have been most considerate and helpful.

Many colleagues have helped guide my research through their discussions and comments. Among these, I wish to thank particularly Drs. J. H. Cahn, M. A. Gordon, L. A. Higgs, K. I. Kellermann, J. M. MacLeod, D. D. Morrison, E. C. Olson, and J. C. Webber.

During the period of preparation of this thesis, I have been supported by a NASA traineeship, an NSF traineeship, and an NSF fellowship. This research has also been supported by NSF Grant GP-8161. The theoretical calculations were performed by the CDC G-20 computer of the Department of Electrical Engineering at the University of Illinois.

TABLE OF CONTENTS

LIST OF TABLES

LIST OF FIGURES

Chapter I

INTRODUCTION

Fifteen years ago passive microwave radiation from Venus was first measured (Mayer, et al., 1958). Nearly one hundred sets of radio observations have now been published, for wavelengths ranging from 0.1 to 70 cm. For these wavelengths, Planck's radiation law can be replaced by the Rayleigh-Jeans approximation, in which the brightness of the source is proportional to the first power of its blackbody temperature. For observations made with a single radio telescope, no significant resolution over the disk of Venus is possible. In the reductions of such observations, the planet is assumed to radiate uniformly over its disk. The measured flux density is then proportional to the disk-averaged brightness temperature, defined as the temperature of a perfect radiator subtending the same solid angle as Venus and emitting the same flux density of radiation at the wavelength of observation. The disk-averaged brightness temperature is often called simply the brightness temperature, and its variation with wavelength defines the radio spectrum of the planet.

The radio spectrum of Venus shows brightness temperatures greater than 500° K for most wavelengths greater than 2 cm. An atmosphereless planet at the distance of Venus from the Sun would have a surface temperature of only 300-

400° K, the exact value depending upon the albedo and rotation rate of the planet. Various theories have been proposed to account for the high observed brightness temperatures. The most plausible one is the greenhouse theory, wherein the atmosphere traps the thermal radiation from the surface and causes the surface and lower atmosphere to attain much higher temperatures than those expected for the case of equilibrium between the planet and its insolation. The entire collection of observations and measurements of Venus, made by ground-based telescopes and various spacecraft, has been best explained by proposing that the Cytherean microwave radiation is entirely thermal. The new models presented in Chapter IV are based upon this assumption, but we will see that the observed radio spectrum of Venus at decimeter wavelengths cannot readily be explained by an entirely thermal origin.

The opacity of the Cytherean atmosphere is roughly proportional to λ^{-2} (Ho, et al., 1966), where λ is the wavelength, due to pressure-induced absorption by CO_2 and other gases. As the wavelength of observation increases, we receive radiation from deeper layers of the atmosphere and subsurface, and the subsurface contribution begins to dominate near the wavelength of the spectral maximum, which is probably near 6 cm (Dickel, 1967). More stringent limits can thus be placed upon the physical properties of the subsurface layers of Venus by improving the accuracy of the

radio spectrum for λ greater than about 6 cm. Cytherean brightness temperature measurements become more difficult as the wavelength of observation increases beyond a few centimeters because (1) the flux density from a thermal source is generally proportional to λ^{-2}, (2) background synchrotron sources become stronger with increasing wavelength, and (3) more confusion sources are encountered for single-dish observations because the beamwidth of an antenna is proportional to λ.

The precision of the brightness temperature derived from any set of observations depends upon how well the radio telescope is calibrated. For λ greater than about 2 cm, the observed planetary flux densities are placed on an absolute basis by adopting a flux density scale for one or more standard celestial sources. The standard source is included in the observing program, and the flux density of the source under investigation is determined by measuring the ratio of the amplitude of the source under investigation to that of the standard source. Because the gain of the telescope receiver fluctuates, the amplitude of a source is usually, in fact, the ratio of the output deflection due to the source to the output deflection due to a signal from a plasma noise tube placed at the extreme front-end of the receiver system. The signal from the plasma noise tube is attenuated so that its output deflection is roughly comparable to the output deflection due to the source.

Both the plasma signal and the attenuation factor must remain unchanged throughout the set of observations. For λ less than about 2 cm, a flux density scale for celestial standard sources has not been established. The absolute calibration is often then performed by comparing the telescope response to a ground-based transmitter with the response of an adjacent, standard-gain horn antenna system. Alternatively, one or more celestial sources, such as Jupiter or the Sun, can be used at the shorter wavelengths as a calibration standard.

Pollack and Morrison (1970) have improved the accuracy of the radio spectrum over the range of 0.2 to 21 cm by including only the best sets of observations in this wavelength range and adjusting the adopted flux densities for the comparison sources, when possible, to conform to the flux density scale of Scheuer and Williams (1968) and Kellermann, et al. (1969). Pollack and Morrison selected only the brightness temperatures published since 1963 with given standard errors less than $\pm 60^{o}$ K and with calibration procedures adequately described by the observers. For $\lambda < 2$ cm, they chose a representative set of published brightness temperatures.

Ten years ago the first unequivocal detection of Venus by radar was made (Muhleman, 1961; Pettengill, et al., 1962). One of the important quantities measurable with a radar system is the planetary cross section, defined as the target

intercept area which, if it were to reradiate isotropically all the incident flux, would yield the echo power actually observed (Pettengill, et al., 1962). For a smooth conducting sphere, the radar cross section equals its geometric cross section. For a non-smooth dielectric sphere, such as a planet, the radar cross section is usually expressed as a percentage of the geometric cross section. At least a dozen sets of reliable cross section measurements have been published, for wavelengths ranging from 3.6 to 784 cm. The radar spectrum will herein be defined as the variation of radar cross section with wavelength.

The purposes of this investigation are to define more accurately the radio spectrum of Venus in the wavelength range of 7 to 15 cm and to interpret the resulting radio spectrum and the radar spectrum in terms of atmospheric and subsurface parameters. New observations at four separate wavelengths are described in Chapter II. In Chapter III, I present the observational radio and radar spectra. Chapter IV contains theoretical results for a two-layer planetary subsurface, i.e., an inner core of dielectric material overlain with a thin epilith characterized by a smaller dielectric constant. Conclusions from all of the observations and model calculations are given in Chapter V.

Chapter II

NEW OBSERVATIONS

A. Observations at ARO

During the period of July 6-9, 1969, observations of Venus at 9.26 cm were conducted at the Algonquin Radio Observatory (ARO) with the 46-meter altazimuth radio telescope of the National Research Council of Canada. A total of $27\frac{1}{2}$ hours of telescope time was used. The observing dates were chosen such that solar interference was minimized. At a phase angle near 282° and separated from the Sun by 44°, Venus was near its maximum western elongation. The phase angle is defined here as the planet-centered angle measured westward from the Sun to the Earth (Dickel, 1966). The telescope was equipped with a tunnel diode amplifier and had a bandwidth of 475 MHz centered on 3240 MHz. The front-end Dicke switch was attached to a reference load at room temperature. For a 60-second integration time, the rms system noise temperature was typically 0.033° K.

While conducting the observations, each of the two source coordinates, right ascension and declination, was found by a peaking-up procedure, which I shall now describe. The slope of the main lobe of the beam pattern for a parabolic antenna is greatest at an angle from the axis of approximately one-half the half-power beamwidth, i.e., where the power response is one-half of the maximum. The

half-power beamwidth for the 46-meter antenna at 9.26 cm was found to be 8.2 arc minutes by making several scans through the point source 3C147. The right ascension of Venus was found first; the telescope coordinates were set at the ephemeris position for Venus and then at the two positions that were at the ephemeris declination and 4 arc minutes from the ephemeris position in right ascension. If the signal levels on the chart recorder were the same for the two positions displaced in right ascension, the ephemeris right ascension was used as the right ascension setting for Venus on the telescope console. If these two signal levels differed, a trial-and-error method was used to find the right ascension setting on the telescope console for which the two signal levels were the same. Once the right ascension setting was determined, the telescope was moved to that right ascension and the declination setting for Venus was then found by an analogous procedure.

Venus and 3C123, the standard comparison source, were both observed by using the on-off technique, in which the signal from the sky background is subtracted from the signal due to the source and the sky background together. The off positions were 3 beamwidths or 24 arc minutes from the source position in each of the four cardinal points. The telescope gain was frequently calibrated by recording an internal signal from a plasma noise tube. The plasma noise tube is usually assumed to be stable over periods of the

order of a few days, and no error analysis concerning it was performed. A typical observing run consisted of a series of 60-second integrations made in the following order: off north, on source, off south, on internal calibration signal, off south, off west, on source, off east. The receiver output was recorded on an analog chart recorder and simultaneously fed to a digital computer for on-line printout. The digital results were normally used in the reductions. The output deflection for a source signal or an internal calibration signal was found by subtracting the mean level of the two adjacent off-integrations from the level of the on-integration. The 60-second duration used for each integration was long enough to provide a good averaging of the noise fluctuations and yet short enough that the observing run was not significantly affected by variations in the telescope system parameters, such as the noise temperature contribution from ground radiation. The average of the two output deflections for the source was divided by the output deflection for the internal calibration signal to give a source amplitude for each observing run.

Each observing run was normally made next to one in an orthogonal plane of polarization, and the source amplitudes from the two were averaged in order to remove the effects of polarization inherent to either the source or the antenna. Let $\bar{A}_{\varphi}$ be the average amplitude for Venus, resulting from two such adjacent observing runs. Let $\bar{A}_{3C123}$ be the average

amplitude for 3C123. Then, if S_{3C123} is the adopted flux density for 3C123, the flux density of Venus is given by

$$S_{\varphi} = S_{3C123} \, (\bar{A}_{\varphi}/\bar{A}_{3C123}). \qquad (1)$$

If a source size is appreciable compared to the beamwidth, the measured source amplitude must be increased by a factor determined by the structures and relative sizes of the source and the beam. No such corrections were required for these observations, made with a beamwidth of 8.2 arc minutes. The angular semi-diameter of Venus was less than 10 arc seconds, and several interferometric source-structure surveys (e.g., Bash, 1968, and Fomalont, 1968) have shown 3C123 to be negligibly small.

The brightness temperature of Venus, T_B, is computed from the following formula:

$$T_B = \frac{\lambda^2 \, S_{\varphi}}{2k(\pi \, \phi^2)} \, , \qquad (2)$$

where λ is the wavelength of observation, k is Boltzmann's constant, and ϕ is the angular semi-diameter of Venus. The value used for $\bar{A}_{3C123}$ in the calculation of each individual value of T_B on a given day usually resulted from the observations of 3C123 made on that day. One measurement of $\bar{A}_{3C123}$ was made each day.

Before the individual brightness temperatures were computed, the raw data were first corrected for systematic errors resulting from (1) faulty telescope pointing,

(2) change of telescope gain as a function of zenith angle, and (3) confusing background sources in the beam. For a few of the integrations during the observing session, the records showed the pointing to be somewhat in error. Corrections, which never exceeded a few per cent, were made for these output deflections on the basis of the known pointing error and a beam assumed to be Gaussian with a half-power width of 8.2 arc minutes.

The source 3C196 was observed twice each day in order to determine the zenith angle dependence of telescope gain and atmospheric attenuation. Not enough observations were made for this procedure to be successful because the error bars for each measurement were too large. However, all of the observations of Venus and 3C123 were corrected for these effects according to a curve derived by Higgs and Purton (1969) for the 46-meter telescope at 9.26 cm. This curve showed only a very weak zenith angle dependence, as one should expect for wavelengths greater than several centimeters. The zenith angle ranges were 28^{o} to 40^{o} for Venus and 27^{o} to 32^{o} for 3C123, and the largest correction required was less than 0.5%.

If background point sources of appreciable strength are in the telescope beam while either on source or off source, the observing program can easily be rendered useless. Point-source surveys by Day, et al. (1966), Dickel, et al. (1967), Gower, et al. (1967), and Höglund (1967) were

examined, and three sources were found to have affected some of the Venus measurements. VRO 17.03.07 was very close to the position of Venus on July 6, and the Venus data from that day were consequently discarded. VRO 17.04.01 and VRO 17.04.02 affected the west and south baselines, respectively, on July 9. The Venus data from that day were salvaged, however, by subtracting only the east and north baselines from the source level instead of the east-west and north-south average baselines.

Although 3C123 is not listed by Kellermann, et al. (1969) as a standard source suitable for calibration, it is a moderately strong source with a well-measured spectrum. The flux density of 3C123 at 3240 MHz was first estimated to be 23.3 f.u. (1 flux unit = 10^{-26} W m^{-2} Hz^{-1}) from a graphical interpolation procedure, using the flux densities listed in Table 1 and plotted in Figure 1.

Table 1

Flux Densities of 3C123

Frequency (MHz)	S_{3C123} (f.u.)	Reference
38	577	Kellermann, et al. (1969)
178	189.0	Kellermann, et al. (1969)
750	72.3	Kellermann, et al. (1969)
1400	45.9	Kellermann, et al. (1969)
2695	27.2	Kellermann, et al. (1969)
5000	16.32	Kellermann, et al. (1969)
8000	10.49	Dent and Haddock (1966)
10630	8.00	Doherty, et al. (1969)

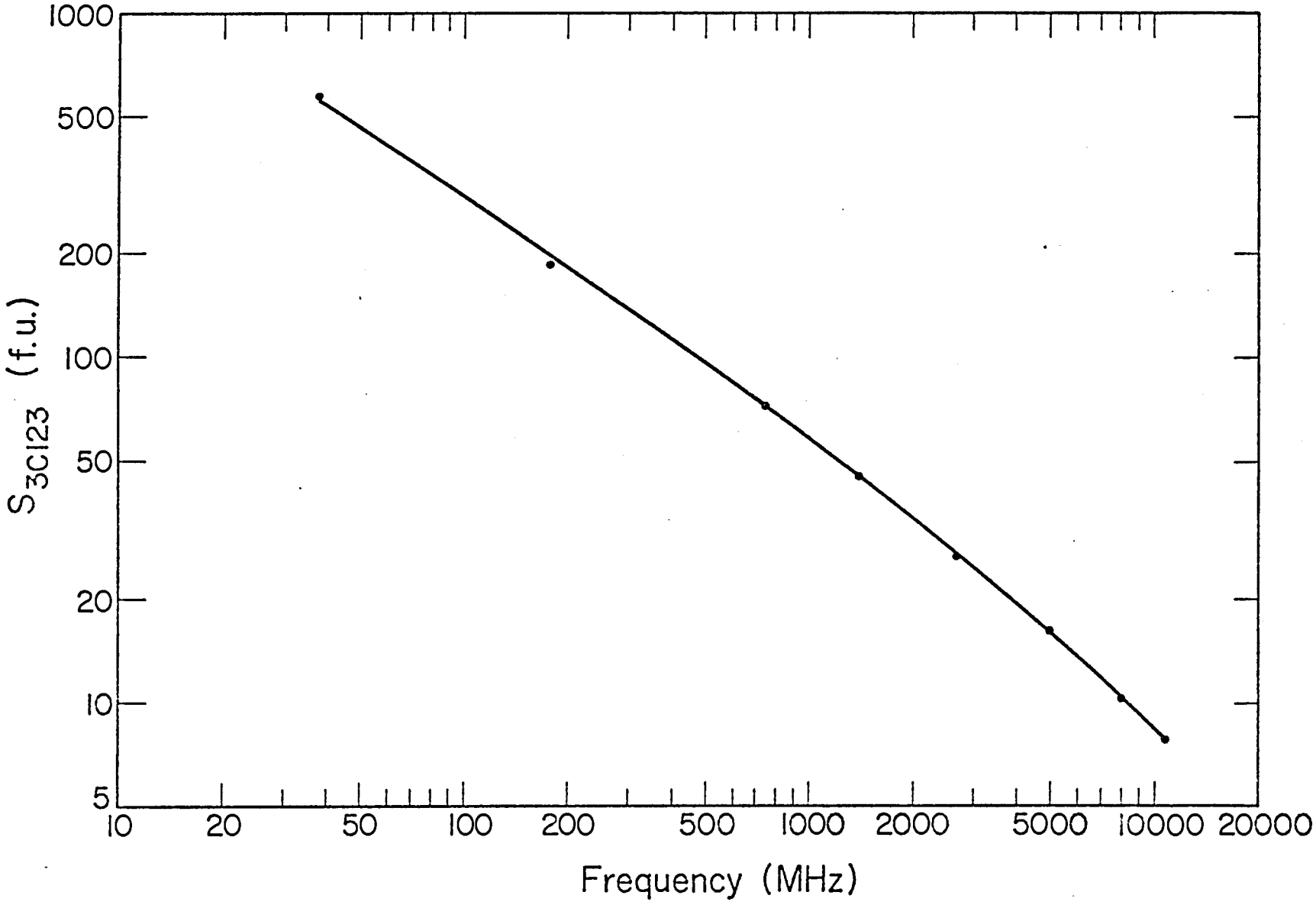

Figure 1. Flux densities of 3C123 vs. frequency. The 8 data points are taken from Table 1. The curve is an "eyeball" fit.

The 8-GHz flux density published by Dent and Haddock (1966) has been revised upward by 7%; Table 1 contains the revised value. This correction factor at 8 GHz results from the use of the absolute flux density measurements of Cassiopeia A at 8.25 and 15.50 GHz by Allen and Barrett (1967) instead of the absolute flux density measurements used originally by Dent and Haddock (1966). In order to relate antenna temperatures to flux densities at 8 GHz, Dent and Haddock used absolute flux density measurements at 9.40 GHz made of Cassiopeia A by Stankevich (1962), of Taurus A by Lazarevskii, et al. (1963), and of Cygnus A by Lastochkin, et al. (1964). The measurements of Cassiopeia A at 8.25 and 15.50 GHz by Allen and Barrett were used by Kellermann, et al. (1969) in their determination of the radio spectrum of this primary standard source.

A second estimate of 25.3 f.u. for the flux density of 3C123 at 3240 MHz was obtained from a flux density of 19.9 f.u. for the standard source 3C218 (Kellermann, et al., 1969) and a value of 0.787 ± 0.020 for the flux density ratio of 3C218 to 3C123 at 3240 MHz measured by the staff at ARO (MacLeod, 1971). This flux density ratio was determined from only three observations of the relative strengths, and no corrections for beam broadening by either 3C123 or 3C218 were made. Several interferometric source-structure surveys (e.g., Bash, 1968, and Fomalont, 1968) have shown 3C218 to be a rather complex source, but small enough relative to an

8-arc minute antenna beam that it could be considered a point source. From the above analysis, the flux density of 3C123 at 3240 MHz was adopted as 24.3 ± 1.6 f.u.

A total of fourteen usable measurements of the brightness temperature were made, and the results are listed in Table 2. Because only the east and north baselines were used on July 9, the brightness temperatures for that day were given $\frac{1}{2}$ weight in computing the mean brightness temperature for the three days of usable observations. When an effective integration time of 30 seconds was assigned to each on-source integration for which only one baseline was used, the total effective integration times for Venus and 3C123 were 45^m and 8^m, respectively.

Table 2

Measurements of Brightness Temperature at ARO

Date	$T_B(^oK)$
7/7/69	711
	689
	713
7/8/69	662
	678
	627
	660
	685
7/9/69	747
	673
	666
	638
	668
	693

The solid angle of Venus was computed by using an angular semi-diameter of 8.41 arc seconds at a distance of one astronomical unit, as given by The American Ephemeris and Nautical Almanac; this value corresponds to a planetary radius of 6100 km. This choice for the planetary radius is justified in Section D of Chapter IV, where the true size of the emitting disk is taken into account. The signal-to-noise ratio during the observing session was such that the standard error for a determination of the ratio of the Venus signal to the internal calibration signal, from a single 60-second integration on Venus, was about 7%. When the value of 24.3 f.u. for the flux density of 3C123 is used, the mean brightness temperature of Venus turns out to be 679^{o} K, with a computed internal standard error of 9^{o} K. When the estimated error in the flux density scale is accounted for, the final brightness temperature is 679 ± 46^{o} K.

For an adopted aperture efficiency of 56% (Higgs, 1970), the internal calibration signal gave an antenna temperature of about 1.84^{o} K. The flux density of Venus was about 0.062 of the flux density of 3C123.

B. Observations at NRAO

During the periods July 16-19, 1970, and July 31-August 2, 1970, the 2-4 GHz tunable receiver of the National Radio Astronomy Observatory (NRAO) was made available for

observations of Venus with the 43-meter equatorial antenna at Green Bank, West Virginia. Seven hours were allotted each day, for a total of 49 hours of telescope time. A different part of the 2-4 GHz range was covered by each of three parametric amplifiers, with some overlap possible. Approximately one hour was needed to change amplifiers in the front-end for operation in a different frequency range, but tuning within the range of each amplifier could be accomplished within a few minutes from the control room.

This tunable receiver was quite advantageous because the subsurface emission from Venus begins to dominate the atmospheric contribution in the 7.5 to 15 cm wavelength range of the receiver. By using a moderately strong standard calibration source, 3C218, having a well-known power-law radio spectrum, and identical observing procedures at a few separate wavelengths within the range of the receiver, I was able to improve the relative and absolute accuracies of the radio spectrum of Venus. The shape of the derived relative radio spectrum of Venus in this critical wavelength range depended mainly upon how well 3C218 fits a power-law spectrum and what spectral index was adopted for this source. The absolute values of the derived brightness temperatures chiefly depended upon the flux density scale adopted for 3C218.

The basic receiver characteristics for each day are given in Table 3. The center frequency, half-power bandwidth,

and center wavelength are given by f_0, B, and λ_0, respectively. ΔT_{rms} represents the typical rms system noise temperature for a 60-second integration time. A reference load at room temperature was used for switching throughout the observations.

Table 3

Receiver Characteristics at NRAO

Date	f_0 (MHz)	B (MHz)	λ_0 (cm)	ΔT_{rms} (^oK)
7/16/70	2100	~46	14.3	0.009
7/17/70	2100	~46	14.3	0.010
7/18/70	3240	83	9.26	0.009
7/19/70	2500	~50	12.0	0.010
7/31/70	2100	46	14.3	0.005
8/ 1/70	3800	80	7.89	0.006
8/ 2/70	3800	82	7.89	0.007

Solar interference was again minimized, since Venus was separated from the Sun by 41^o and 44^o during the first and second observing sessions, respectively. These separations correspond to respective phase angles of Venus of 68^o and 75^o.

For the 43-meter telescope at a wavelength of 11 cm, Altenhoff (1968) has derived empirical pointing correction curves, which allow the observer to calculate indicated source coordinates from the true coordinates as functions of hour angle and declination. From observations of 3C218, Orion A, and M17, these curves were found to be accurate enough for this research and were used for all of the Venus observations. However, the telescope coordinates

for the calibration standard, 3C218, were determined by the peaking-up procedure used at ARO.

The on-off observing technique was again used, but with some slight modifications. The off positions were 30 arc minutes from the source position for each observing wavelength. A typical observing run consisted of a series of 60-second integrations made in the following order: on source, off west, on source, off east, on source, off south, on source, off north, on source, off west, on internal calibration signal, off west. The integration times for 3C218 were usually 30 seconds.

The total-power output of the receiving system was continuously monitored by one channel of the analog chart recorder, in addition to the switched-power output of the Dicke switch on the other channel. Abrupt changes in the total-power output occurred several times during the observations, most of these changes occurring when the telescope position was changed. Only for a part of these abrupt changes did there appear to be a simultaneous change in the switched-power output. These changes were thought to have been caused possibly by water in one or more of the telescope cables.

When abrupt changes in the total-power output occurred while re-positioning the telescope, the adjacent baseline was not used in determining the immediate source output deflection. Only on July 19 did abrupt changes in the

total-power output occur during integration periods, and the data from these particular integration periods were not used. Source output deflections determined from the baseline on only one side were given $\frac{1}{2}$ weight in computing the source amplitude for each observing run.

The angular semi-diameter of Venus was again less than 10 arc seconds, and 3C218 is also quite small compared to an antenna beam with a half-power width of 8 arc minutes or more. Both Venus and 3C218 were taken to be point sources relative to the beamwidths used at NRAO. For beamwidths of a few arc minutes, perhaps a small source-size correction for 3C218 would be appropriate.

The remaining reduction procedures were analogous to those used for the ARO data. The observing records showed only one telescope pointing error, and a 3% correction was made for the respective source output deflection. The gain of an equatorial telescope is generally considered to be a function of both hour angle and declination. For small meridian angles, the telescope gain can usually be treated as a function of only the zenith angle. No gain curves applicable to these observations had been previously derived, and none could be determined from the observations themselves because of insufficient accuracy in the individual measurements. However, for the wavelengths employed in these observations and zenith angles less than 60°, no significant variations in telescope gain or in atmospheric attenuation

as functions of zenith angle are expected, and no corresponding corrections were made. The zenith angle ranges for all observations used in the final reductions were 28^{o} to 59^{o} for Venus and 50^{o} to 60^{o} for 3C218. The sky surrounding Venus during the observations was apparently devoid of any confusion sources of appreciable strength, as none could be found in the known, applicable point-source surveys, by Day, et al. (1966) and Gower, et al. (1967).

The individual brightness temperatures for each wavelength are listed in Table 4. The flux densities adopted for 3C218 were taken from the radio spectrum given for it by Kellermann, et al. (1969) and are listed in column 7 of Table 5, which summarizes the results of the observations. The other columns are described below:

col. 1: λ = wavelength of observation.

col. 2: N_{φ} = total number of measurements of the brightness temperature, with each measurement including one observing run in a known plane of polarization and a following run in an orthogonal plane of polarization.

col. 3: t_{φ} = total effective integration time for Venus.

col. 4: N_{3C218} = total number of measurements of the ratio of the 3C218 signal to the internal calibration signal, with each measurement including a run in each of two orthogonal planes of polarization.

col. 5: t_{3C218} = total effective integration time for 3C218.

col. 6: Error = typical error for the ratio of the Venus signal to the internal calibration signal, from a single 60-second integration.

Table 4

Measurements of Brightness Temperature at NRAO

λ = 7.89 cm		λ = 9.26 cm		λ = 12.0 cm		λ = 14.3 cm	
Date	T_B(^oK)	Date	T_B(^oK)	Date	T_B(^oK)	Date	T_B(^oK)
8/1/70	565	7/18/70	746	7/19/70	584	7/16/70	566
	666		649		689		816
	721		643		856		698
	742		710		783		721
	584		627		662		715
8/2/70	707				632		630
	752						651
	764					7/17/70	777
	693						765
	662						758
	735						780
	671					7/31/70	630
	660						617
							585
							585
							679
							624
							621
							637
							581
							640

Table 5

Final Results for NRAO Observations

λ (cm)	N_{φ}	t_{φ} (min)	N_{3C218}	t_{3C218} (min)	Error (%)	S_{3C218} (f.u.)	$\frac{S_{\varphi}}{S_{3C218}}$	T_B (^oK)	σ_i (^oK)	σ_t (^oK)
7.89	13	101	3	13	6.0	17.2	0.109	686	17	38
9.26	5	43	1	4½	5.6	19.9	0.054	675	23	41
12.0	6	43½	1	4½	8.2	25.2	0.027	701	41	54
14.3	21	176½	5	26¼	9.3	29.5	0.017	670	16	37

col. 8: S_{φ}/S_{3C218} = ratio of flux density of Venus to flux density of 3C218. S_{φ} corresponds to the mean angular semi-diameter of Venus during the observations.

col. 9: T_B = mean brightness temperature of Venus.

col. 10: σ_i = computed internal standard error for T_B.

col. 11: σ_t = total standard error for T_B, including a 5% error assigned to S_{3C218}.

Some important telescope parameters are given in Table 6, the columns of which are described as follows:

col. 1: λ = wavelength of observation.

col. 2: HPBW = estimated half-power beamwidth.

col. 3: T_{cal} = antenna temperature of internal calibration signal, measured in laboratory by the staff of NRAO.

col. 4: ϵ_{ap} = calculated aperture efficiency.

Table 6

Telescope Parameters for NRAO Observations

λ (cm)	HPBW (arc min)	T_{cal} ($^{\circ}$K)	ϵ_{ap} (%)
7.89	7.9	4.4	15½
9.26	9.3	4.4	40
12.0	12.0	5.6	52
14.3	14.3	5.7	48

Chapter III

THE OBSERVATIONAL SPECTRA

Extensive compilations of known brightness temperature measurements have been published by Barrett and Staelin (1964), Kuzmin (1967), Dickel (1967), and Barber and Gent (1967). At the time these papers were written, Venus was believed to exhibit a significant phase effect. A few sets of observations had seemed to indicate that the brightness temperature of Venus reached a maximum near inferior conjunction. Subsequent observations of higher quality by Epstein, et al. (1968), Morrison (1969a), and Dickel, et al. (1968) have shown that Venus has essentially no phase variation at wavelengths of 0.34, 1.94, and 4.52 cm, respectively. A reasonable conclusion is that the microwave phase effect of Venus is nonexistent.

The 23 points in the observational radio spectrum of Pollack and Morrison (1970) are reproduced in Table 7, with a revision at 4.52 cm and eight additions. Dickel, et al. (1968) adopted a flux density of 12.3 f.u. for 3C123 at 4.52 cm (6630 MHz). From the graphical interpolation procedure described in Section A of Chapter II, a value of 12.5 f.u. appears to be a better choice. This results in a revised brightness temperature of $665 \pm 30^{\circ}$ K for Venus.

The final uncertainties given by Pollack and Morrison for the derived brightness temperatures for $\lambda \geq 1.94$ cm

were assigned somewhat subjectively (Morrison, 1969b), in order to account for consistency in the flux density ratios of comparison sources, for whether or not the comparison sources were good standards as defined by Kellermann, et al. (1969), and for the internal errors published by the observers. These three factors have also been considered in assigning uncertainties to the eight additional points. Although the internal error for the 9.26-cm temperature measured at ARO was only 9^{o} K, the comparison source used, 3C123, is not defined by Kellermann, et al. (1969) as a good standard. The error for this entry in Table 7 was set at 30^{o} K to account for the inconsistency in the determination of the flux density of 3C123 at 9.26 cm. Because the comparison source used at NRAO, 3C218, is a good standard, the computed internal standard errors for the four temperatures reported in Section B of Chapter II were used in Table 7. Stankevich (1970) did not state whether or not the published error of 35^{o} K in his measurement at 11.1 cm was internal or total; hence, it was left unchanged. For $\lambda >$ 21.4 cm, Kellermann (1966) and Hardebeck (1965) have conducted the only sets of observations that meet the selection criteria of Pollack and Morrison, excluding the wavelength requirement. The errors published by Kellermann (1966) and Hardebeck (1965) were considered to be representative and were left unchanged.

Table 7

The Observational Radio Spectrum of Venus

λ (cm)	Given T_B (°K)	Calibration Standards	Derived T_B (°K)	References and Notes	
0.225	235^{+40}_{-}	Jupiter	240^{+40}_{-}	Efanov, et al. (1969)	
0.340	296^{+20}_{-}	Sun	296^{+30}_{-}	Epstein, et al.(1968)	a
0.815	375^{+60}_{-}	Jupiter	380^{+40}_{-}	Efanov, et al. (1969)	
0.85	380^{+50}_{-}	Moon, 3C144	350^{+40}_{-}	Lynn, et al. (1964)	
0.86	425^{+40}_{-}	Absolute	425^{+40}_{-}	Kalaghan, et al. (1968)	
1.18	400^{+36}_{-}	Moon	400^{+36}_{-}	Law & Staelin (1968)	a
1.43	451^{+40}_{-}	Moon	451^{+40}_{-}	Law & Staelin (1968)	a
1.46	595^{+50}_{-}	Absolute	440^{+50}_{-}	Griffith, et al.(1967)	
1.58	477^{+57}_{-}	Moon	477^{+57}_{-}	Law & Staelin (1968)	a
1.94	495^{+35}_{-}	3C274	495^{+25}_{-}	Pollack & Morrison(1970)	
3.12	553^{+21}_{-}	3C123 & others	592^{+40}_{-}	Berge & Greisen (1969)	
3.75	675^{+35}_{-}	3C274,3C353	675^{+20}_{-}	Klein (1970)	
4.52	653^{+15}_{-}	3C123	665^{+30}_{-}	Dickel, et al. (1968)	b
6.0	630^{+30}_{-}	3C123,3C274,3C348	650^{+40}_{-}	Hughes (1966)	
6.0	706^{+45}_{-}	3C218	725^{+30}_{-}	Dickel (1967)	
6.0	700^{+45}_{-}	3C353	700^{+35}_{-}	Pollack & Morrison(1970)	
7.5	617^{+18}_{-}	3C48,3C196	630^{+30}_{-}	Berge & Greisen (1969)	
7.89	686^{+38}_{-}	3C218	686^{+17}_{-}	This thesis	c
9.26	679^{+46}_{-}	3C123	679^{+30}_{-}	This thesis	c
9.26	675^{+41}_{-}	3C218	675^{+23}_{-}	This thesis	c
10.0	622^{+20}_{-}	3C123	640^{+35}_{-}	Drake (1964)	
10.6	580^{+30}_{-}	3C48	650^{+40}_{-}	Clark & Kuzmin (1965)	
11.1	710^{+35}_{-}	3C218	710^{+35}_{-}	Stankevich (1970)	c
11.3	620^{+20}_{-}	3C218	630^{+20}_{-}	Kellermann (1966)	
12.0	701^{+54}_{-}	3C218	701^{+41}_{-}	This thesis	c
14.3	670^{+37}_{-}	3C218	670^{+16}_{-}	This thesis	c
21.2	591^{+25}_{-}	3C218	587^{+25}_{-}	Davies & Williams (1966)	
21.3	590^{+20}_{-}	3C218	590^{+20}_{-}	Kellermann (1966)	
21.4	528^{+33}_{-}	3C123,3C348,3C353	515^{+30}_{-}	Drake (1964)	
31.2	510^{+50}_{-}	3C218	510^{+50}_{-}	Kellermann (1966)	c
70.	518^{+40}_{-}	~50 sources	518^{+40}_{-}	Hardebeck (1965)	c

a. Calibration standard listed by Pollack and Morrison (1970) has been revised here to conform with that given in the reference.

b. Derived T_B of Pollack and Morrison (1970) has been revised here.

c. These points are additions to the spectrum given by Pollack and Morrison (1970).

The absolute calibrations of the temperatures of Venus found by Stankevich at 11.1 cm, Kellermann at 31.2 cm, and Hardebeck at 70 cm were deemed to be correct as published. Conway, et al. (1963) and Kellermann (1964) established flux density scales which were widely used before the recent scale of Kellermann, et al. (1969) was published. As discussed by Kellermann, et al. (1969), some recent low-frequency measurements are in closer agreement with the Kellermann (1964) scale than with the scale of Conway, et al., which is lower than Kellermann's scale by 8% at 38 and 178 MHz. Kellermann, et al. (1969), however, retained the scale of Conway, et al. for $\lambda > 40$ cm, because it has been so widely used and because large uncertainties in the low-frequency calibration still exist. Stankevich's adopted flux density for 3C218 agrees with the power-law spectrum published for this source by Kellermann, et al. (1969), and the flux density adopted by Kellermann (1966) for 3C218 at 31.2 cm is in satisfactory agreement with the scales of both Kellermann (1964) and Kellermann, et al. (1969). Hardebeck (1965) employed about 50 radio sources, with flux densities based on the scale of Kellermann (1964), for his calibration.

The derived brightness temperatures from Table 7 are plotted versus wavelength on a logarithmic abscissa scale in Figure 2. The shape of the spectrum for $\lambda \geq 6$ cm should be best indicated by the several temperature measurements using 3C218 as a calibration standard. The new brightness

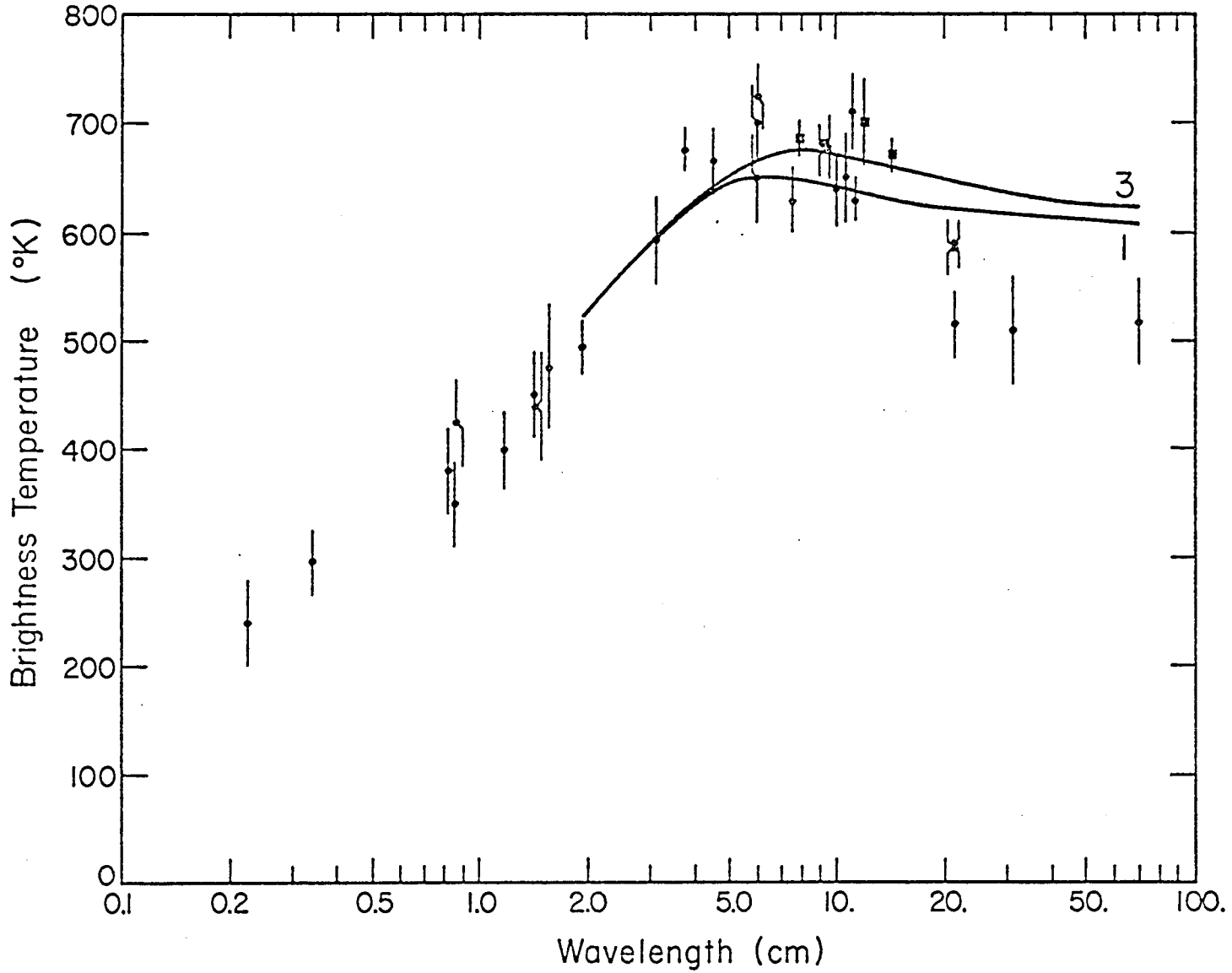

Figure 2. Radio spectra of Venus. The 31 data points are taken from Table 7, with the square points representing the new brightness temperatures presented in Chapter II of this thesis. The curves marked 1 and 3 are the theoretical spectra for models 1 and 3 from Table 9.

temperatures reported in Chapter II of this thesis reveal that the radio spectrum of Venus is rather flat at temperatures of 670-700° K in the region from 6 to 14 cm, with a maximum near 6 cm. There is, however, a discrepancy at 11 cm. Both Kellermann (1966) at 11.3 cm and Stankevich (1970) at 11.1 cm used the 64-meter telescope of the Commonwealth Scientific and Industrial Research Organization at Parkes, Australia, and 3C218 as a calibration standard, but their error bars in Figure 2 are separated by 25° K. At wavelengths longer than 14 cm, the data show a precipitous decline in the spectrum as λ increases from 14 to 31 cm.

The 12 radar spectral points listed by Muhleman (1969) are reproduced in Table 8 and plotted in Figure 3. Each value of η, the radar cross section, is followed by its standard error.

Table 8

The Observational Radar Spectrum of Venus

λ (cm)	Date	η (%)	References and Notes	
3.6	1964	0.9 ± 0.5	Karp, et al. (1964); Evans (private communication to Muhleman (1969))	
3.8	1964-65	1.7 ± 0.3	Evans (1968)	a
12.5	1961	11.2 ± 2.0	Muhleman (1963)	
12.5	1964	11.4 ± 1.0	Carpenter (1964)	
23.0	1964	15.2 ± 1.0	Evans, et al. (1965)	
41.0	1962	15.0 ± 3.0	Kotelnikov, et al. (1962)	
41.0	1964	19.0 ± 3.0	Kotelnikov (1965)	
68.0	1961	13.1 ± 2.0	Pettengill (1962)	b
70.0	1964	15.0 ± 1.0	Dyce & Pettengill (1966)	
600	1962	20.0 ± 10.0	Klemperer, et al. (1964)	
784	1962	15.0 ± 4.0	James & Ingalls (1964)	
784	1964	13.0 ± 4.0	James, et al. (1967)	

a. Reflectivity revised from 1% (Evans, et al., 1966).
b. Reflectivity revised by Evans, et al. (1965).

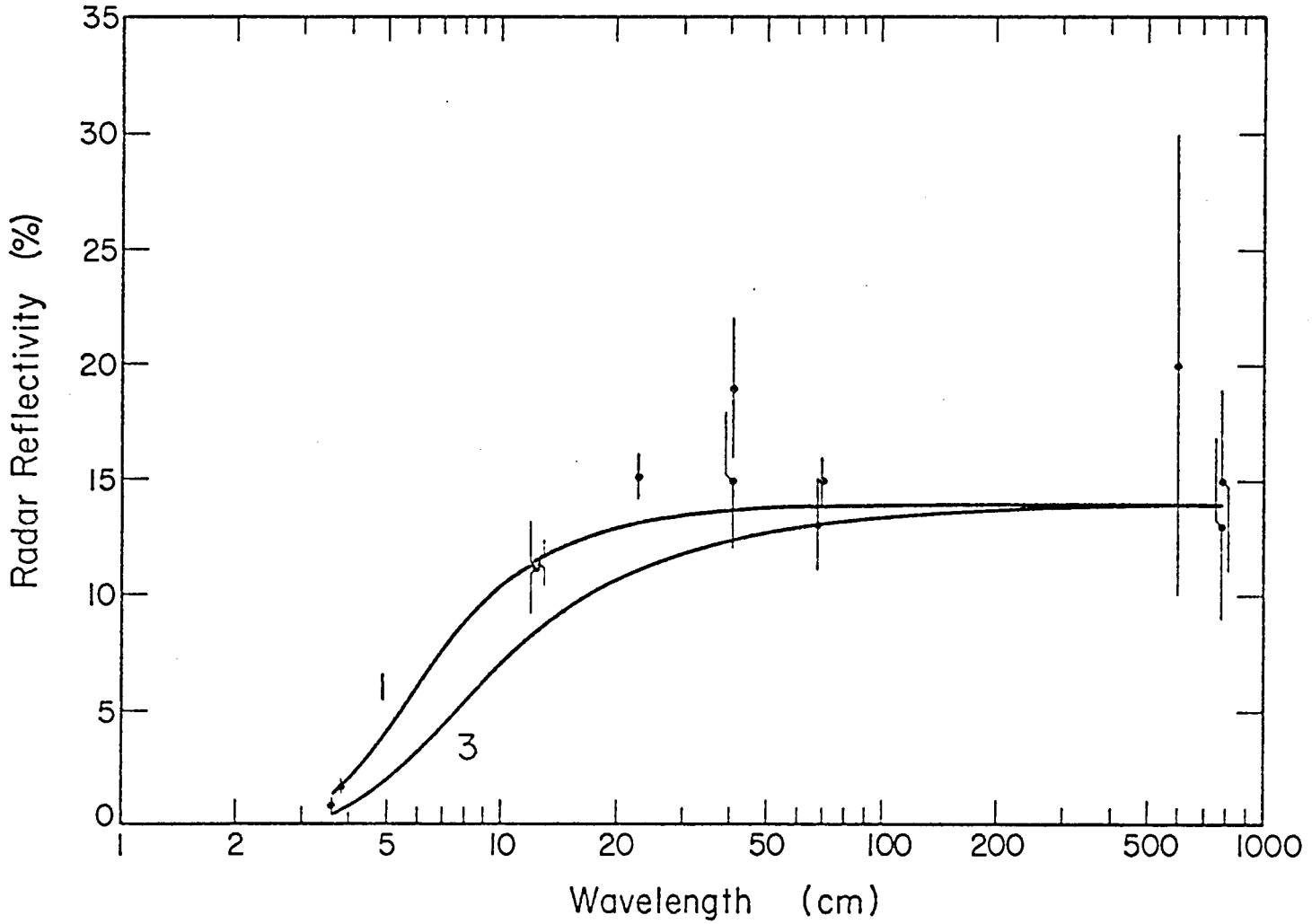

Figure 3. Radar spectra of Venus. The 12 data points are taken from Table 8. The curves marked 1 and 3 are the theoretical spectra for models 1 and 3 from Table 9.

Chapter IV

THEORETICAL MODELS

A. Subsurface Theory

Most attempts to explain the radio and radar spectra of Venus have dealt with variations of atmospheric parameters and employed a dielectric sphere as a subsurface model. Strelkov (1967), however, attempted to explain the smaller brightness temperatures at decimeter wavelengths and the smaller radar reflectivities at centimeter wavelengths by introducing a two-layer subsurface model. He assumed a layer of hard rock overlain with a thin layer of material of low density. Such an outer layer is not uncommon among terrestrial planets, and the name regolith is usually given to it. Johnson (1968) pointed out, though, that the term regolith should be used only for a layer of disintegrated rock fragments which include soil. His suggested alternative term, epilith, will be used in this dissertation.

Strelkov was able to match many of the observations reported before 1967 with epilith depths of a few meters, but he assumed that the Cytherean atmosphere exhibited no opacity for wavelengths greater than 5 cm. In addition, he used a subsurface thermometric temperature of only 670° K. The American fly-by mission, Mariner 5, and the four Soviet spacecraft performing <u>in situ</u> experiments, Veneras 4,5,6, and 7, have unequivocally confirmed the earlier interpretation

of the microwave data from ground-based observations that the atmosphere makes a very considerable contribution to the radiation at a wavelength of 5 cm, and that the surface temperature is near 750° K (e.g., Avduevsky, et al., 1971). Tikhonova and Troitskii (1969) have presented a more complete theory of radiation from a two-layer subsurface model, in an attempt to explain lunar microwave radiation. Unlike Strelkov, they included a term for inward-moving radiation emitted by the epilith material and a correction factor for multiple reflections at the boundaries of the epilith. The portion of the theory of Tikhonova and Troitskii relevant to Venus is presented below and then combined with a theory of the atmospheric radiation, taken from Ho, et al. (1966), to predict radio and radar spectra.

Consider the two-layer medium shown in Figure 4, in which the upper and lower layers are characterized by the dielectric constants ϵ_1 and ϵ_2 ($> \epsilon_1$), respectively. The plane-parallel approximation is used, and the dielectric constant of the atmosphere is taken to be unity. The origin of the depth coordinate, y, is the surface, which is herein defined as the interface between the subsurface and the atmosphere. We seek the intensity of the radiation moving outward from the surface and making an angle θ with the normal to the surface. Angles θ_1 and θ_2 are related to θ via Snell's law of refraction.

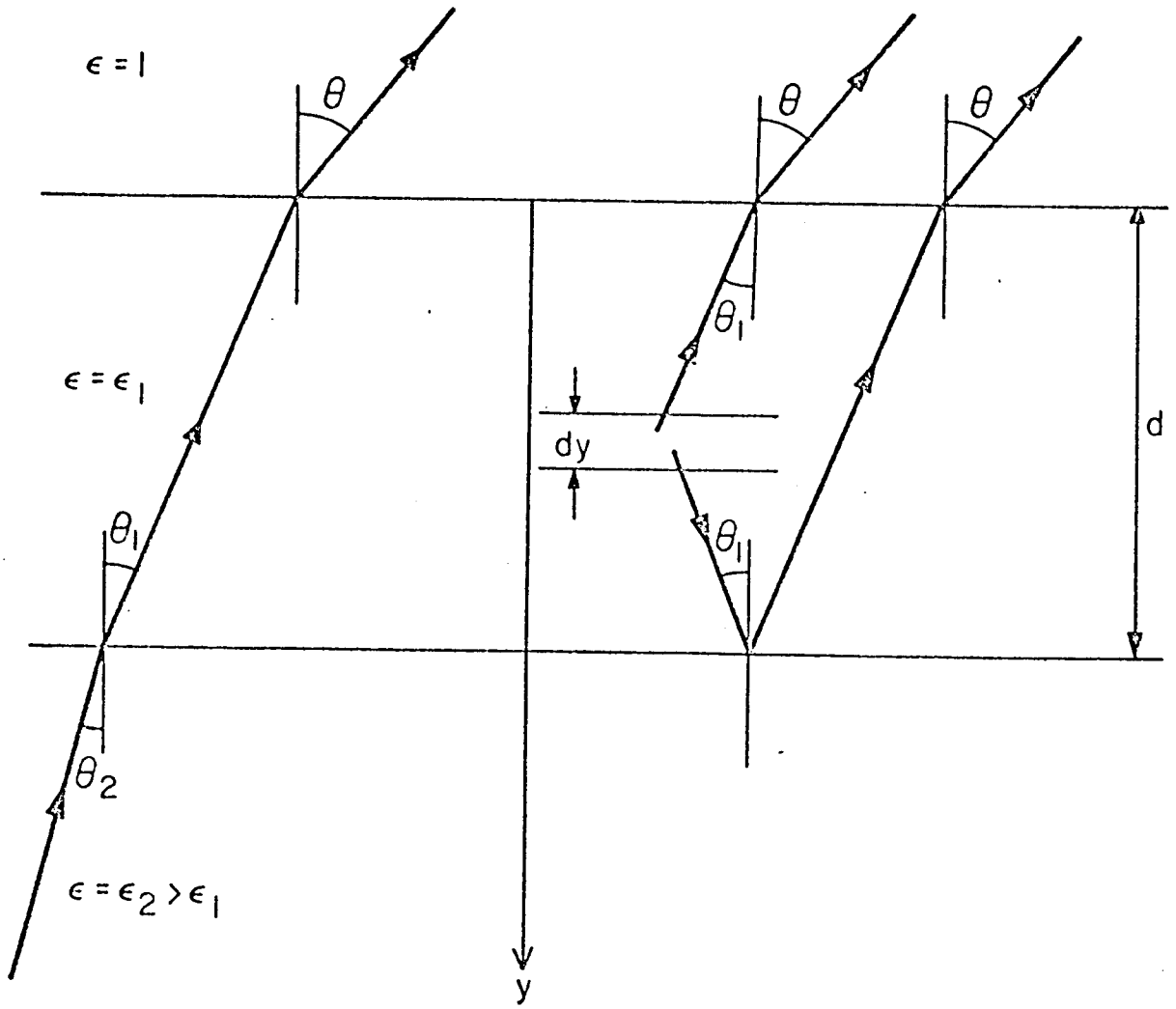

Figure 4. Two-layer subsurface model, taken from Tikhonova and Troitskii (1969).

The outward radiation intensity can be expressed as

$$I(0) = I_1(0) + I_2(0) \quad , \tag{3}$$

where $I_1(0)$ is the intensity from the epilith of thickness d, incorporating multiple reflections at the boundaries, and $I_2(0)$ is the intensity from the semi-infinite lower layer, also incorporating multiple relfections at the boundaries of the epilith. Local thermodynamic equilibrium is assumed to exist throughout the medium. The term $I_2(0)$ can be written as

$$I_2(0) = D^2 \, I_2(d) \quad , \tag{4}$$

where $I_2(d)$ is the intensity of radiation incident from below upon the epilith and D^2 is the transmission coefficient for the passage of the radiation through the epilith. The thermometric temperature of the subsurface material is taken to be constant with depth and time and equal to the surface temperature, T_s. Using the Rayleigh-Jeans approximation for Planck's radiation law in the formal solution to the equation of radiative transfer,

$$I_2(d) = (2k/\lambda^2) \, T_s, \tag{5}$$

where k is Boltzmann's constant. The intensity $I_2(d)$ is attenuated during its passage to the surface because of partial reflections at the boundaries of the epilith and absorption by the epilith material. The transmission coefficient D^2 is actually an infinite sum because of

multiple reflections within the epilith (Tikhonova and Troitskii, 1969), but it can readily be evaluated and is given by

$$D^2 = \frac{(1-R_1)(1-R_2)\, e^{-\tau_e \sec\theta_1}}{1+R_1R_2\, e^{-2\tau_e \sec\theta_1} + 2\sqrt{R_1R_2}\, e^{-\tau_e \sec\theta_1} \cos\left(\frac{4\pi\sqrt{\epsilon_1}}{\lambda} d \sec\theta_1\right)}, \quad (6)$$

where R_1 and R_2 are the mean Fresnel reflection coefficients at the surface and at the lower boundary of the epilith, respectively, and τ_e is the optical depth of the epilith.

The term $I_1(0)$ can be written as

$$I_1(0) = I_{1,out}(0) + I_{1,in}(0) , \quad (7)$$

where $I_{1,out}(0)$ is the intensity at the surface of radiation emitted by the epilith in the outward direction, and $I_{1,in}(0)$ is the intensity of radiation emitted by the epilith in the inward direction and reaching the surface because of reflection at the lower boundary of the epilith. Applying the radiative transport solutions given by Tikhonova and Troitskii to the case of constant temperature, we find

$$I_{1,out}(0) = (2kT_s/\lambda^2) \frac{D^2\, e^{+\tau_e \sec\theta_1}}{(1-R_2)} (1-e^{-\tau_e \sec\theta_1}), \quad (8)$$

and

$$I_{1,in}(0) = (2kT_s/\lambda^2) \frac{D^2\, R_2}{(1-R_2)} (1-e^{-\tau_e \sec\theta_1}). \quad (9)$$

The reflection coefficient, R, from the two-layer medium for radiation incident from above at an angle θ can be derived by a procedure similar to that used in computing D^2. We find that

$$R=\frac{R_1+R_2\ e^{-2\tau_e \sec\theta_1}+2\sqrt{R_1R_2}\ e^{-\tau_e \sec\theta_1}\cos\left(\frac{4\pi\sqrt{\epsilon_1}}{\lambda}d\sec\theta_1\right)}{1+R_1R_2\ e^{-2\tau_e \sec\theta_1}+2\sqrt{R_1R_2}\ e^{-\tau_e \sec\theta_1}\cos\left(\frac{4\pi\sqrt{\epsilon_1}}{\lambda}d\sec\theta_1\right)}. \quad (10)$$

Equations 6 and 10 show an oscillatory, or interference, term which contains the factor cos(z), where

$$z = \frac{4\pi\sqrt{\epsilon_1}}{\lambda}\, d \sec\theta_1. \quad (11)$$

The argument z depends upon both the wavelength and the depth of the epilith. Consider D^2 as a function of z only and average it over an interval in z of 2π, with the probability density of z taken as a constant over the interval (cf. Hagfors, 1970). The average transmission coefficient is then

$$\overline{D^2} = \frac{(1-R_1)(1-R_2)\ e^{-\tau_e \sec\theta_1}}{1-R_1R_2\ e^{-2\tau_e \sec\theta_1}}. \quad (12)$$

A similar averaging of R gives

$$\overline{R} = \frac{R_1+R_2\ e^{-2\tau_e \sec\theta_1}-2\ R_1R_2\ e^{-2\tau_e \sec\theta_1}}{1-R_1R_2\ e^{-2\tau_e \sec\theta_1}}. \quad (13)$$

Tikhonova and Troitskii (1969) obtained their average coefficients by simply equating the interference term to zero. These averages simplify the computations and become

more realistic as the receiver bandwidth and epilith depth increase. Since we receive a band of frequencies, there is always an instrumental averaging of D^2 and R. Also, there would most assuredly be variations in depth d for the epilith of a real planet.

B. Atmospheric Theory

Ho, et al. (1966) measured the coefficients of induced absorption by CO_2, N_2, A, and Ne in the temperature range 240-500° K to pressures as high as 130 atm. They also studied the absorption due to small amounts of water vapor in N_2, over the temperature interval 393-473° K, and over a comparable pressure range. All of their measurements were made at 9260 MHz. Because the microwave region lies on the low-frequency wing of both the translational and rotational spectra, the microwave induced absorption coefficient is proportional to the square of the frequency. Their absorption coefficient is

$$\alpha = (P/P_s)^2 \, (x/\lambda^2) \, (273/T)^5 \ \mathrm{cm}^{-1}, \qquad (14)$$

where

$$x = P_s^{\,2}(15.7 f_{CO_2}^2 + 3.90 f_{CO_2} f_{N_2} + 2.64 f_{CO_2} f_A + 0.085 f_{N_2}^2 + 1330 . f_{H_2O}) \, (10^{-8}), \qquad (15)$$

P is the pressure in atmospheres, P_s is the surface pressure, λ is the wavelength in cm, T is Kelvin temperature,

and f_{CO_2}, f_{N_2}, f_A, and f_{H_2O} represent the molar fractions of carbon dioxide, nitrogen, argon, and water vapor. For my new model calculations, the coefficient of f_{H_2O} was increased by a factor of 1.55 (Pollack and Morrison, 1970).

Ho, et al. gave in their equation 19 the integrals needed for the computation of brightness temperatures of Venus for the case of a one-layer subsurface. Their atmospheric model consists of a lower layer in adiabatic equilibrium with a constant temperature lapse rate and an upper isothermal layer. The atmosphere is considered to be an ideal gas in hydrostatic equilibrium. The opacities of the adiabatic and isothermal layers are given respectively by

$$\tau_a = \left(\frac{x}{\lambda^2}\right)\left(\frac{273}{T_S}\right)^5\left(\frac{\mathcal{R}T_S}{\bar{\mu}g}\right)\left(\frac{\gamma}{\gamma-1}\right)\left(\frac{1-\xi^s}{s}\right) \qquad (16)$$

and

$$\tau_i = \left(\frac{x}{\lambda^2}\right)\left(\frac{273}{T_S}\right)^5\left(\frac{\mathcal{R}T_C}{\bar{\mu}g}\right)\left(\frac{\xi^{s-1}}{2}\right) \quad , \qquad (17)$$

where λ is the wavelength in cm, $\mathcal{R}$ is the universal gas constant, $\bar{\mu}$ is the mean molecular mass, g is the acceleration due to gravity, γ is the ratio of specific heat capacities, T_C is the temperature in the isothermal layer, $\xi = T_C/T_S$, and $s = (2\gamma/(\gamma-1))-4$. In calculating the intensities of the radiation resulting from atmospheric emission and absorption, local thermodynamic equilibrium is assumed and the plane-parallel approximation is used.

C. Some Recent Interpretations of the Observational Spectra

Pollack and Morrison (1970) have performed a thorough investigation of the Cytherean atmosphere by comparing various detailed theoretical spectra with their observational radio spectrum and the observational radar spectrum given by Muhleman (1969). Assuming the microwave radiation from Venus to be derived solely from thermal emission, Pollack and Morrison used a combination of the data from Veneras 4, 5, and 6 (Avduevsky, et al., 1968, 1970) and Mariner 5 (Kliore, et al., 1969) to arrive at temperature and pressure profiles for the atmosphere above a height of 20 km. For the lowest 20 km they initially used an adiabatic profile and then experimented with the possibility of an isothermal layer extending from the surface to various heights above the surface. Their initial estimate of the carbon dioxide molar abundance was 90%, resulting from measurements by Mariner 5 (Kliore, et al., 1969) and by Veneras 4, 5, and 6 (Avduevsky, et al., 1968, 1970). Nitrogen, water vapor, and dust were assumed to be the only other sources of atmospheric opacity. The coefficients for nonresonant absorption by CO_2, N_2, and H_2O vapor were taken from the laboratory results of Ho, et al. (1966); a correction factor of 1.55 was applied to the water vapor coefficient. This correction factor is necessary because Ho, et al. measured the nonresonant absorption coefficient

of the water in a nitrogen environment. Carbon dioxide has a greater pressure-broadening ability. Effects due to the resonant absorption by water vapor near a wavelength of 1.35 cm were also taken into account.

The principle constraints used by Pollack and Morrison in determining acceptable atmospheric models were (1) $T_B(1.94\text{ cm}) = 495 \pm 35^\circ$ K, (2) $T_B(6.0\text{ cm}) = 690 \pm 50^\circ$ K, (3) $T_B(21\text{ cm}) = 575 \pm 50^\circ$ K, and (4) $\tau(3.8\text{ cm}) = 1.0 \pm 0.1$, where τ is the normal opacity (i.e., for $\theta=0$) of the Cytherean atmosphere. They concluded that CO_2 is not the only source of microwave opacity in the atmosphere, and that H_2O vapor was more likely than dust to be a constituent of the Cytherean troposphere and provide the necessary additional opacity. If it is H_2O vapor that provides the additional opacity, its molar abundance would be $0.65 \pm 0.35\%$. They also found that an isothermal layer in the lowest 20 km of the atmosphere could have a thickness of no more than 4 km. The surface temperature and pressure were estimated to be $770 \pm 25^\circ$ K and 95 ± 20 atm.

Although Pollack and Morrison provided generally good fits to the radio spectrum in the range of 0.2 to 21 cm, their theoretical temperatures near the spectral maximum were not as high as some of the temperatures listed in their observational radio spectrum. Likewise, the new temperatures reported in Chapter II of this dissertation exceed their theoretical temperatures. In addition, several

temperatures near 500° K for $\lambda > 30$ cm were not included by them because of the large errors associated with these observations, and their theoretical temperatures for these wavelengths were about 600° K. An attempt to eliminate the first of these two shortcomings is described in the next two sections.

Muhleman (1969) used the radar spectrum to estimate the normal opacity of the Venus atmosphere as a function of wavelength and to estimate the mean dielectric constant of the subsurface material of Venus. The radar cross section, η, also called the radar reflectivity, at a given wavelength is a function of the electromagnetic reflectivity of the subsurface material of Venus, the normal opacity of the atmosphere of Venus, and the roughness of the surface of Venus at that wavelength. Muhleman assumed that η_s, the reflectivity that would be observed for an atmosphereless Venus, is constant as a function of wavelength. The normal atmospheric opacity was assumed to vary inversely with the square of the wavelength. The water vapor line at 1.35 cm has little effect upon the opacity of the atmosphere at the wavelengths for which the radar cross section has been measured. Using the best estimates for the backscattering law in his least-squares regression analysis on the observed values of η, Muhleman concluded that the normal optical depth was best represented by $\tau(\lambda) = (1.01 \pm 0.04)\ (3.8/\lambda)^2$, where the wavelength is in centimeters. His best estimate for η_s, the

surface reflectivity, was 15.10±0.64%. The surface reflectivity may be written as the product of $\bar{\rho}$, the mean reflection coefficient of the subsurface, and G, the gain or directivity of the surface. The mean reflection coefficient depends upon the electromagnetic reflectivity of the subsurface material and is defined as the ratio of the total scattered power to the total incident power, i.e., the radar albedo averaged over a hemisphere. The gain is the ratio of the power per unit solid angle scattered back toward the radar to the average power per unit solid angle scattered in all directions. The gain is unity for a smooth, isotropically reflecting sphere and is, in general, a function of the size and distribution of surface irregularities. The surface gain of Venus is rather uncertain, but using an estimated value of 1.08 and taking the solid part of Venus to be a homogeneous dielectric, Muhleman found the subsurface to be characterized by a dielectric constant of 4.80±0.30.

D. New Models

Using the theory from Sections A and B of Chapter IV, with $\overline{D^2}$ substituted for D^2 in equations 4, 8, and 9, we can write down integrals for the seven separate contributions to the brightness temperature:

$$T_{B,1} = 2\,T_s \int_0^1 (1-R_2)\, e^{-\tau_e/\mu_1} (1-R_1) C_{mr}\, e^{-(\tau_a+\tau_i)/\mu}\, \mu\, d\mu, \quad (18)$$

$$T_{B,2} = 2\,T_s \int_0^1 (1-e^{-\tau_e/\mu_1})(1-R_1) C_{mr}\, e^{-(\tau_a+\tau_i)/\mu}\, \mu\, d\mu, \quad (19)$$

$$T_{B,3}=2T_s \int_0^1 (1-e^{-\tau_e/\mu_1})R_2\, e^{-\tau_e/\mu_1}(1-R_1)C_{mr}\, e^{-(\tau_a+\tau_i)/\mu}\, \mu\, d\mu, \quad (20)$$

$$T_{B,4}=2T_s \int_0^1 \int_0^1 \left[(1-\xi^s)\psi+\xi^s\right]^{1/s} e^{-(\tau_i+\psi\tau_a)/\mu}\, \tau_a\, d\psi\, d\mu, \quad (21)$$

$$T_{B,5}=2T_s \int_0^1 \int_0^1 \left[(1-\xi^s)\psi+\xi^s\right]^{1/s} \bar{R}\, e^{-[\tau_i+\tau_a(2-\psi)]/\mu}\tau_a\, d\psi\, d\mu, \quad (22)$$

$$T_{B,6}=T_c \left[1-2\int_0^1 e^{-\tau_i/\mu}\, \mu\, d\mu\right], \quad (23)$$

and

$$T_{B,7}=2T_c \int_0^1 (1-e^{-\tau_i/\mu})\, \bar{R}\, e^{-(2\tau_a+\tau_i)/\mu}\, \mu\, d\mu, \quad (24)$$

where C_{mr} = the correction for multiple reflections within the epilith = $(1-R_1R_2\exp(-2\tau_e/\mu_1))^{-1}$, $\mu = \cos(\theta)$, $\mu_1 = \cos(\theta_1)$, $\psi = \tau/\tau_a$, and τ is a variable of integration. The first term, $T_{B,1}$, accounts for the emission from the lower, semi-infinite subsurface layer. The second and third terms represent outward and inward emission, respectively, from the epilith. The fourth and sixth terms account for the outward emission from the adiabatic and isothermal atmospheric layers, respectively, and the fifth and seventh terms represent the inward emission from these layers which is reflected from the subsurface material. The third term, which was not included by Strelkov (1967), amounted to more than 2% of the total brightness temperature at some wavelengths for some of the new models considered in this dissertation. The correction for multiple reflection was

found to increase the theoretical brightness temperatures for the new models by less than 1%. No corrections for refraction in the Cytherean atmosphere were made. All the theoretical computations were done with the aid of a CDC G-20 computer, and numerical quadrature subroutines were used to evaluate the integrals in the brightness temperature calculations.

In computing observed brightness temperatures of Venus, one customarily finds its solid angle by using an angular semi-diameter of 8.41 arc seconds at one astronomical unit, which corresponds to a planetary radius of 6100 km. The radius of Venus determined by radar is about 6050 km (Ash, et al., 1968). Hence, for wavelengths at which the opacity of the atmosphere is very small, the observed brightness temperatures are 1-2% too small (Pollack and Morrison, 1970). Instead of correcting all of the published results for this effect, I have multiplied my theoretical brightness temperatures by a correction factor, C_{sd}. The mean level of radiation from Venus is designated as the height above the surface at which the optical depth is unity. The effective radius, r_{eff}, is taken to be equal to the radar radius. Then

$$C_{sd} = (r_{eff}/6100)^2 \ , \tag{25}$$

and

$$T_B = C_{sd} \sum_{j=1}^{7} T_{B,j} \ . \tag{26}$$

Campbell and Ulrichs (1969) have experimentally investigated the electrical properties of many terrestrial rocks at frequencies of 450 MHz and 35 GHz. They found that ϵ and tan Δ, the loss tangent, for each of the rocks were essentially the same at both frequencies and showed little variation for temperatures ranging from 300° K to ~875° K. The absorption lengths were found to be proportional to the wavelength. For tan $\Delta \ll 1$, the absorption coefficient for these terrestrial rocks can be represented by

$$\kappa = \frac{2\pi \sqrt{\epsilon} \tan \Delta}{\lambda} \quad . \tag{27}$$

In view of our complete lack of knowledge about the composition of the Cytherean subsurface, I assume that the absorption coefficient for it follows equation 27. Both ϵ_1 and tan Δ_1, the loss tangent for the epilith, are assumed to be wavelength-independent. Consequently, we can write

$$\tau_e = \frac{2\pi \sqrt{\epsilon_1} \tan \Delta_1 \, d}{\lambda} \quad . \tag{28}$$

As the density of terrestrial rocks is decreased, the dielectric constant generally decreases, and there have been several attempts to find an expression by which the two properties can be related (e.g., Campbell and Ulrichs, 1969). For this research, only a rough approximation is necessary, and I have used the following convenient expression given by Krotikov (1962):

$$\sqrt{\epsilon} = 1 + a\rho \quad , \tag{29}$$

where ρ is the density in g cm^{-3}, and $a = 0.5$ $cm^3 g^{-1}$. Campbell and Ulrichs (1969) also found that the loss tangent is nearly proportional to the density. For this research, I assume that $\tan \Delta/\rho = 0.006$, a value adopted by Morrison (1970) in a study of the planet Mercury. Thus, once a value for ϵ_1 is chosen, a corresponding value for $\tan \Delta_1$ can be calculated through the two density relationships.

The Cytherean surface is taken to be a smooth sphere for all of the new theoretical results presented in this dissertation. The theoretical radar reflectivity, R^*, is found by evaluating $\bar{R}$ for $\theta = 0$ and multiplying the result by an exponential attenuation factor due to atmospheric absorption. After simplification, we find

$$R^* = \left[1 - \frac{(4\sqrt{\epsilon_1})(F_1 - F_3\, e^{-2\tau_e})}{(F_1F_2 - F_3F_4\, e^{-2\tau_e})} \right] e^{-2(\tau_a + \tau_i)} \quad , \tag{30}$$

where

$$F_1 = (\sqrt{\epsilon_2/\epsilon_1} + 1)^2 \quad ,$$

$$F_2 = (\sqrt{\epsilon_1} + 1)^2 \quad ,$$

$$F_3 = (\sqrt{\epsilon_2/\epsilon_1} - 1)^2 \quad ,$$

and

$$F_4 = (\sqrt{\epsilon_1} - 1)^2 \quad .$$

For the case in which $\epsilon_2 = \epsilon_1$ and $\tau_a = \tau_i = 0$, equation 30 reduces to the familiar result for a semi-infinite dielectric slab,

$$R^* = \left(\frac{\sqrt{\epsilon_1} - 1}{\sqrt{\epsilon_1} + 1}\right)^2 . \qquad (31)$$

E. Results

The main purpose of these new model calculations is to determine whether the two-layer subsurface model will provide a better fit to the radio spectrum at the greater wavelengths, but within the constraints imposed by the radar spectrum. Pollack and Morrison (1970) have employed an elaborate atmospheric model to determine atmospheric parameters from the radio and radar spectra. Many of their conclusions were based upon their fits to the radio spectrum for $\lambda < 2$ cm, and thus their detailed atmospheric model was both justified and necessary. However, my results will be based upon fits to the spectra for $\lambda > 2$ cm, and some simplification of the atmospheric model appears to be justified.

My "standard" atmospheric model is similar to that of Pollack and Morrison (1970). The molar abundance of CO_2 for my models is taken to be 90%, with the remainder consisting of H_2O vapor and N_2. For this composition, they concluded that the water vapor abundance would be between 0.35% and 1.5%; their final estimate was 0.65 ± 0.35%.

Pollack and Morrison note that the amounts of water vapor detected by the Venera spacecraft (Vinogradov, et al., 1970) correspond to molar abundances ranging from 0.4% to 2.5%. I have used a value of 0.4% for all of my models. For an adiabatically extrapolated model of the lowest 20 km of the atmosphere, Pollack and Morrison arrived at a surface temperature and pressure of 758° K and 91.6 atm. From a preliminary analysis of the Venera 7 data, Avduevsky, et al. (1971) concluded that the surface temperature and pressure is 747±20° K and 90 atm in the region of the Venera 7 landing area, and that the temperature lapse rate over at least the first 50 km above the surface is close to a value of -8.6° K km^{-1}. The bottom of the visible cloud layer on Venus is apparently about 60 km above the surface (e.g., Avduevsky, et al., 1970). A surface temperature of 758° K and a lapse rate of -8.6° K km^{-1} for the first 60 km are adopted; the temperature in the isothermal region for my models is 242° K. A surface pressure of 91.6 atm is adopted. The acceleration due to gravity is taken to be 878 cm sec^{-2}.

Pollack and Morrison accounted for the resonant part of the absorption coefficient for water vapor, due to the 1.35-cm line. This line has very little effect on my analysis and was consequently neglected. The atmospheric parameters adopted above and the subsurface parameters adopted below were assumed to apply for the entire surface area of the planet. This assumption appears to be justified by the

interferometric results of Sinclair, et al. (1970), who found no large-scale differences in the surface temperature greater than 25° K at a wavelength of 11.1 cm. Hall and Branson (1971), observing Venus with an interferometer at 6 cm, found the total-power contour map of the planetary disk to be essentially circularly symmetric, but having a bright feature on the dark side of the planet with a brightness temperature $50 \pm 25^{\circ}$ K greater than the mean disk temperature. Neither the magnitude nor the location of the feature could be fully explained by the authors with the help of plausible local changes in the subsurface or atmospheric parameters. No estimate of the size of this feature was given.

My "standard" atmospheric model gives a value of 1.24 for the ratio of specific heat capacities, assumed constant with height, and results in an opacity of 1.03 at 3.8 cm. For $\epsilon_2 = \epsilon_1 = 4.8$, my theoretical brightness temperatures agree with those of Pollack and Morrison to within ~2% for $\lambda > 2$ cm. The major part of this discrepancy is probably due to my neglect of refraction, but my main concern is the differential effect of the two-layer subsurface models upon the spectra for $\lambda > 2$ cm.

Let us consider equation 30 for two more special cases. If $\tau_a = \tau_i = 0$ and $\tau_e \to \infty$,

$$R^* = \left(\frac{\sqrt{\epsilon_1} - 1}{\sqrt{\epsilon_1} + 1}\right)^2 . \qquad (32)$$

If $\tau_a = \tau_i = 0$ and $\tau_e = 0$,

$$R^* = 1 - \frac{4\sqrt{\epsilon_1 \epsilon_2}}{(\epsilon_1 + \sqrt{\epsilon_2})(1 + \sqrt{\epsilon_2})} . \qquad (33)$$

I have assumed that $\tau_e \propto 1/\lambda$. Hence, an atmosphereless planet would reflect like a semi-infinite slab with dielectric constant ϵ_1 for very small wavelengths, and like a semi-infinite slab with an effective dielectric constant determined by ϵ_1 and ϵ_2 for very large wavelengths. Depending upon the values chosen for ϵ_1, ϵ_2, and d, this effect will result in perturbations of different sizes upon the radio and radar spectra computed for no variation of ϵ within the subsurface. As pointed out in Section C of Chapter IV, several observed brightness temperatures near the peak in the radio spectrum are higher than those predicted by previous models, and the observed brightness temperatures for $\lambda > 30$ cm are significantly lower than the previous theoretical temperatures. By using a low effective dielectric constant for $\lambda \simeq 6$ cm and a high effective dielectric constant for $\lambda > 30$ cm, we can see that the two-layer model holds some promise in explaining the observations. However, these effective dielectric constants would lower the radar spectrum for small wavelengths and raise it for large wavelengths, and the error bars associated with the observational radar reflectivities must be recognized.

The input parameters for nine new models are presented in Table 9, along with some selected results. Models 1, 4,

and 7 have no depth dependence of ϵ and are thus similar to most of the previous models of the Cytherean subsurface. For the two-layer models, I have chosen a value of 1.5 for ϵ_1 and the two values 50 cm and 100 cm for d. The results presented here can generally be reproduced for other small values of ϵ_1 and appropriate corresponding values for d and ϵ_2. Three representative values of ϵ_2 have been chosen, such that R^* will approach values of 14.0%, 15.1%, and 17.0% as $\lambda \to \infty$. The compositions of the lower and upper subsurface layers are assumed to be the same. The difference in the dielectric constant of the two layers is assumed to be caused by a difference in density. The density of the lower layer is readily determined by using equation 29. Muhleman (1969) deduced a surface reflectivity, η_s, of 15.1% and a value of 14.0% for the reflectivity after an estimate for the surface gain had been taken into account. For my model of a smooth surface, a reflectivity of 17.0% is considered to be consistent with the upper limits of the radar observations. A few selected temperatures and reflectivities for these six two-layer models are given in Table 9, along with the results for the three models having no depth dependence of ϵ. The values of 4.80, 5.16, and 5.78 for ϵ at all depths have been chosen to give reflectivities of 14.0%, 15.1%, and 17.0% for $\lambda \to \infty$. The spectra for models 1 and 3 are compared with the observational spectra in Figures 2 and 3. These figures clearly show how the

two-layer subsurface model changes the forms of the theoretical spectra computed for the case of a one-layer subsurface.

Table 9

Some Results for Nine New Models

Model No.	ϵ_1	ϵ_2	d (cm)	λ(cm) of Peak T_B	Peak T_B (^oK)	T_B (70cm) (^oK)	R* (3.6cm) (%)	R* (3.8cm) (%)	R* (12.5 cm) (%)	R* (784cm) (%)
1	4.80	4.80	0	6.8	650	610	1.40	1.77	11.5	13.9
2	1.5	6.86	50	7.6	664	620	0.83	1.08	9.9	13.9
3	1.5	6.86	100	8.2	673	624	0.51	0.68	8.5	13.9
4	5.16	5.16	0	6.4	647	602	1.52	1.92	12.5	15.1
5	1.5	7.39	50	7.2	661	612	0.90	1.16	10.7	15.1
6	1.5	7.39	100	7.6	671	616	0.55	0.73	9.2	15.0
7	5.78	5.78	0	6.2	643	590	1.71	2.16	14.1	17.0
8	1.5	8.31	50	6.8	657	600	1.00	1.30	12.0	17.0
9	1.5	8.31	100	7.4	667	604	0.61	0.81	10.3	16.9

Chapter V

CONCLUSIONS, EXPLANATIONS, AND SUGGESTIONS

A. Conclusions from the New Models

The subsurface theory presented in this dissertation is recognized to be highly idealistic and only applies to an average over the entire surface of Venus. The values used for ϵ_1 and ϵ_2 mainly represent differences in the porosity of the subsurface layers and give no information concerning the composition of the subsurface. The values used for ϵ_2 in the models for which $d > 0$ are, however, typical of the dielectric constants of unpulverized terrestrial rocks (Campbell and Ulrichs, 1969).

Examination of Table 9 shows that the peak brightness temperature in the radio spectrum is about 25^{o} K higher for models having an epilith depth of 100 cm than for those having no variation of ϵ with depth. However, for the 100-cm epiliths, the brightness temperatures at 70 cm are increased by about 15^{o} K and the radar reflectivities at centimeter wavelengths are decreased rather markedly. Because the opacity of the epilith, τ_e, has been assumed to vary as λ^{-1}, it is impossible for the effective dielectric constant to change from a low value to a high value for only a one-decade change in wavelength, from 7 to 70 cm. For reasons pointed out in Chapter I, the values of T_B observed near 7 cm wavelength are more reliable than

those for $\lambda > 30$ cm, and more attention was thus paid to obtaining a better fit to the radio spectrum near its peak.

My attempt to improve the fit of theoretical radio and radar spectra to the observational spectra shows that some unknown sources of opacity or some non-thermal emission mechanisms are needed to explain all of the microwave observations of Venus. My two-layer subsurface models do allow a somewhat better fit to the observed radio spectrum near its peak, but only at the expense of worsening the fit to the observed radar spectrum at centimeter wavelengths. The two-layer subsurface theory, in the form presented in this thesis, does not seem to be capable of fitting the low observed brightness temperatures at decimeter wavelengths. In addition, the high atmospheric pressure at the surface of Venus probably does not allow the existence of a highly-porous upper subsurface layer.

The inconsistency resulting from my improvement of the radio fit and simultaneous worsening of the radar fit stems partly from the large uncertainties in the radio and radar data at many wavelengths and from my neglect of the effects of surface roughness. The roughness of the Cytherean surface has not been measured with high accuracy, and the theoretical treatment of the effects of surface roughness upon my two-layer subsurface models would be rather complex.

The measured radar reflectivities refer to surface areas that are small compared to the planetary disk. Perhaps if the measured radar reflectivities at centimeter wavelengths were averaged over the entire surface area of Venus, they would be smaller than the published values and thus agree more closely with some of my theoretical spectra for two-layer subsurface models. As an example of the variability of the radar measurements, consider the cross section at 3.8 cm listed in Table 8, resulting from a revision by Evans (1968) after a more critical error analysis. Even after his revision, there remained some individual data points which were ~100% greater than the mean and, of course, some points smaller than the mean. Evans attributed these fluctuations to variations in the nature of the terrain visible to the radar system (e.g., reflectivity, roughness, and perhaps height).

B. Explanations of the Observed Radio Spectrum at Decimeter Wavelengths

Because Strelkov (1967) neglected the Cytherean atmosphere and used a subsurface thermometric temperature of only 670° K, his two-layer dielectric subsurface models cannot be considered as representative of the Cytherean subsurface and are not a full explanation of the observed radio spectrum at decimeter wavelengths. The two-layer dielectric subsurface

may be considered as one of a class of models which predict a frequency dependence of the radiation capability of the solid portion of the planet. Other examples of this class are (1) a subsurface with a frequency-dependent dielectric constant and thus a frequency-dependent emissivity and (2) a subsurface with a frequency-dependent emissivity due to effects of surface roughness. Both of these models may have some similarity to the Cytherean subsurface at decimeter wavelengths, where the radio spectrum turns sharply downward. Ho, et al. (1966) stated that proper theoretical treatment of the roughness on the scale of a few centimeters tends to lower the brightness temperature at the greater wavelengths.

A better fit to the radio spectrum for $\lambda > 30$ cm would be possible, with no additional changes to the radar spectrum, if we assumed a large decrease in the subsurface temperature over the first meter or two below the surface. As λ increased, the opacity of the subsurface material would decrease. This would cause the effective subsurface temperature to decrease, and the brightness temperature contributions from the subsurface would show a corresponding decline. However, one finds it very difficult to explain how such a subsurface temperature variation could exist, in view of the thick overlying atmosphere. The constant subsurface temperature, T_S, used in the model calculations is much more plausible.

Another possible explanation for the observed decrease in the Cytherean brightness temperature at decimeter

wavelengths would be the presence of a cold, frequency-selective absorber in the atmosphere. If this absorber were transparent at centimeter wavelengths, but became optically thick at decimeter wavelengths, it would reduce both the observed brightness temperatures and the observed radar cross sections at decimeter wavelengths, from what they would be without this absorber. Kuzmin (1964, 1967) proposed that the Cytherean ionosphere is acting as an absorber in this fashion. However, measurements made with the Mariner V spacecraft show that the Cytherean ionosphere may not be dense enough to produce the amount of absorption that is required. The daytime peak electron density is only 5.2×10^5 cm^{-3}, at a height of 135-140 km (Herman, et al., 1971). Further study in this area is needed.

C. Suggestions for Future Research

More high-quality measurements of the radio and radar spectra of Venus at decimeter wavelengths are needed in order to discriminate further among the various models of the subsurface of Venus. In addition, a good measurement of the radar cross section at a wavelength near 6 cm would be particularly valuable. McAdam (1971) of the University of Sydney of Australia has gathered some 408-MHz radio data which should be noteworthy after they are reduced. Perhaps there will be some dedicated observational efforts

made with antennas having diameters on the order of 100 meters. An exciting alternative would be a spacecraft orbiting Venus and equipped with radiometers tuned to the greater wavelengths. Passive observations from such a close range would provide valuable information concerning the subsurface properties of Venus and allow these properties to be mapped as functions of position on the planet. This orbiting spacecraft could also be used in bistatic radar experiments, in which signals from the spacecraft are reflected from the Cytherean subsurface and received on Earth. These experiments would allow an accurate separation of the surface reflectivity into the mean reflection coefficient of the subsurface and the gain of the surface (Green, 1968).

LIST OF REFERENCES

Allen, R. J. and Barrett, A. H. (1967). Absolute Measurements of the Radio Flux from Cassiopeia A and Taurus A at 3.64 and 1.94 cm. Astrophys. J. 149, 1.

Altenhoff, W. J. (1968). NRAO Report-Available at 43-Meter Telescope.

Ash, M. E., Ingalls, R. P., Pettengill, G. H., Shapiro, I. I., Smith, W. B., Slade, M. A., Campbell, D. B., Dyce, R. B., Jurgens, R., and Thompson, T. W. (1968). The Case for the Radar Radius of Venus. J. Atm. Sci. 25, 560.

Avduevsky, V. S., Marov, M. Ya., and Rozhdestvensky, M. K. (1968). Model of the Atmosphere of the Planet Venus Based on Results of Measurements made by the Soviet Automatic Interplanetary Station Venera 4. J. Atm. Sci. 25, 537.

Avduevsky, V. S., Marov, M. Ya., and Rozhdestvensky, M. K. (1970). A Tentative Model of the Venus Atmosphere Based on the Measurements of Veneras 5 and 6. J. Atm. Sci. 27, 561.

Avduevsky, V. S., Marov, M. Ya., Rozhdestvensky, M. K., Borodin, N. F., and Kerzhanovich, V. V. (1971). Soft Landing of Venera 7 on the Venus Surface and Preliminary Results of Investigations of the Venus Atmosphere. J. Atm. Sci. 28, 263.

Barber, D. and Gent, H. (1967). The Brightness Temperature of Venus at 49.1 cm Wavelength. Planet. Space Sci. 15, 907.

Barrett, A. H. and Staelin, D. H. (1964). Radio Observations of Venus and the Interpretations. Space Sci. Rev. 3, 109.

Bash, F. N. (1968). Brightness Distributions of Radio Sources at 2695 MHz. Astrophys. J. Suppl. 16, 373.

Berge, G. L. and Greisen, E. W. (1969). High-Resolution Interferometry of Venus at 3.12-cm Wavelength. Astrophys. J. 156, 1125.

Campbell, M. J. and Ulrichs, J. (1969). Electrical Properties of Rocks and Their Significance for Lunar Radar Observations. J. Geophys. Res. 74, 5867.

Carpenter, R. L. (1966). Study of Venus by cw Radar -- 1964 Results. Astron. J. 71, 142.

Clark, B. G. and Kuzmin, A. D. (1965). The Measurement of the Polarization and Brightness Distribution of Venus at 10.6-cm Wavelength. Astrophys. J. 142, 23.

Conway, R. G., Kellermann, K. I., and Long, R. J. (1963). The Radio Frequency Spectra of Discrete Radio Sources. Mon. Not. R. Astron. Soc. 125, 261.

Davies, R. D. and Williams, D. (1966). Observations of the Continuum Emission from Venus, Mars, Jupiter and Saturn at 21.2 cm Wavelength. Planet. Space Sci. 14, 15.

Day, G. A., Shimmins, A. J., Ekers, R. D., and Cole, D. J. (1966). The Parkes Catalogue of Radio Sources, Declination Zone 0^{o} to $+20^{o}$. Australian J. Phys. 19, 35.

Dent, W. A. and Haddock, F. T. (1966). The Extension of Non-Thermal Radio-Source Spectra to 8000 Mc/s. Astrophys. J. 144, 568.

Dickel, J. R. (1966). Measurement of the Temperature of Venus at a Wavelength of 3.75 cm for a Full Cycle of Planetary Phase Angles. Icarus 5, 305.

Dickel, J. R. (1967). 6-cm Observations and the Microwave Spectrum of Venus. Icarus 6, 417.

Dickel, J. R., Warnock, W. W., and Medd, W. J. (1968). Lack of Phase Variation of Venus. Nature 220, 1183.

Dickel, J. R., Yang, K. S., McVittie, G. C., and Swenson, G. W., Jr. (1967). A Survey of the Sky at 610.5 MHz. II. The Region between Declinations $+15^{o}$ and $+22^{o}$. Astron. J. 72, 757.

Doherty, L. H., MacLeod, J. M., and Purton, C. R. (1969). Flux Densities of Radio Sources at a Wavelength of 2.8 cm. Astron. J. 74, 827.

Drake, F. D. (1964). Microwave Observations of Venus, 1962-1963. Astron. J. 69, 62.

Dyce, R. B. and Pettengill, G. H. (1966). Unpublished.

Efanov, V. A., Kislyakov, A. G., Moiseev, I. G., and Naumov, A. I. (1969). Radio Emission of Venus and Jupiter at 2.25 and 8 mm. Astron. Zh. 46, 147. (Eng. transl.: Sov. Astron.-AJ 13, 110 (1969)).

Epstein, E. E., Oliver, J. P., Soter, S. L., Schorn, R. A., and Wilson, W. J. (1968). Venus: On an Inverse Variation with Phase in the 3.4-mm Emission during 1965 through 1967. Astron. J. 73, 271.

Evans, J. V. (1968). Variations in the Radar Cross Section of Venus. Astron. J. 73, 125.

Evans, J. V., Brockelman, R. A., Henry,J. C., Hyde, G. M., Kraft, L. G., Reid, W. A., and Smith, W. W. (1965). Radio Echo Observations of Venus and Mercury at 23 cm Wavelength. Astron. J. 70, 486.

Evans, J. V., Ingalls, R. P., Rainville, L. P., and Silva, R. R. (1966). Radar Observations of Venus at 3.8-cm Wavelength. Astron. J. 71, 902.

Fomalont, E. B. (1968). The East-West Structure of Radio Sources at 1425 MHz. Astrophys. J. Suppl. 15, 203.

Gower, J. F. R., Scott, P. F., and Wills, D. (1967). A Survey of Radio Sources in the Declination Ranges -07° to 20° and 40° to 80°. Mem. R. Astron. Soc. 71, 49.

Green, P. E., Jr. (1968). Radar Measurements of Target Scattering Properties. In Radar Astronomy (Evans, J. V. and Hagfors, T., eds.), McGraw-Hill Book Co., New York, p. 11.

Griffith, P. H., Thornton, D. D., and Welch, W. J. (1967). The Microwave Spectrum of Venus in the Frequency Range 18-36 Gc/sec. Icarus 6, 175.

Hagfors, T. (1970). Remote Probing of the Moon by Infrared and Microwave Emissions and by Radar. Radio Sci. 5, 189.

Hall, R. W. and Branson, N.J.B.A. (1971). High Resolution Radio Observations of the Planet Venus at a Wavelength of 6 cm. Mon. Not. R. Astron. Soc. 151, 185.

Hardebeck, H. E. (1965). Radiometric Observations of Venus and Mars at 430 Mc/s. Astrophys. J. 142, 1696.

Herman, J. R., Hartle, R. E., and Bauer, S. J. (1971). Models of the Venus Ionosphere. In Planetary Atmospheres, I.A.U. Symposium No. 40 (Sagan, C., Owen, T. C., and Smith, H. J., eds.), D. Reidel Pub. Co., Dordrecht-Holland, p. 23.

Higgs, L. A. (1970). Private Communication.

Higgs, L. A. and Purton, C. R. (1969). Private Communication.

Ho, W., Kaufman, I. A., and Thaddeus, P. (1966). Laboratory Measurement of Microwave Absorption in Models of the Atmosphere of Venus. J. Geophys. Res. 71, 5091.

Höglund, B. (1967). Pencil-Beam Survey of Radio Sources Between Declinations +18° and +20° at 750 and 1410 MHz. Astrophys. J. Suppl. 15, 61.

Hughes, M. P. (1966). Planetary Observations at a Wavelength of 6 cm. Planet. Space Sci. 14, 1017.

James, J. C. and Ingalls, R. P. (1964). Radar Observations of Venus at 38 Mc/sec. Astron. J. 69, 19.

James, J. C., Ingalls, R. P., and Rainville, L. P. (1967). Radar Echoes from Venus at 38 Mc/sec. Astron. J. 72, 1047.

Johnson, D. L. (1968). Lunar Soil: Should This Term Be Used? Science 160, 1258.

Kalaghan, P. M., Wulfsberg, K. N., and Telford, L. E. (1968). Observations of the Phase Effect of Venus at 8.6-mm Wavelength. Astron. J. 73, 969.

Karp, D., Morrow, W. E., Jr., and Smith, W. B. (1964). Radar Observations of Venus at 3.6 Centimeters. Icarus 3, 473.

Kellermann, K. I. (1964). The Spectra of Non-Thermal Radio Sources. Astrophys. J. 140, 969.

Kellermann, K. I. (1966). The Thermal Radio Emission from Mercury, Venus, Mars, Saturn, and Uranus. Icarus 5, 478.

Kellermann, K. I., Pauliny-Toth, I. I. K., and Williams, P. J. S. (1969). The Spectra of Radio Sources in the Revised 3C Catalogue. Astrophys. J. 157, 1.

Klein, M. J. (1970). Private Communication to Pollack and Morrison (1970).

Klemperer, W. K., Ochs, G. R., and Bowles, K. L. (1964). Radar Echoes from Venus at 50 Mc/sec. Astron. J. 69, 22.

Kliore, A., Cain, D., Fjeldbo, G., and Rasool, S. (1969). Structure of the Atmosphere of Venus Derived from Mariner 5 S-Band Measurements. Space Research IX, North-Holland Pub. Co., Amsterdam.

Kotelnikov, V. A. (1965). Radar Observations of Venus in the Soviet Union in 1964. J. Res. NBS, 69D, Radio Sci., 1634.

Kotelnikov, V. A., Dubrovin, V. M., Kislik, M. D., Korenberg, E. B., Minashin, V. P., Morozov, V. A., Nikit-skii, N. I., Petrov, G. M., Rzhiga, O. N., and Shakhovskoi, A. M. (1962). Radar Observations of the Planet Venus. Dokl. Akad. Nauk. SSSR 145, 1035. (Eng. transl.: Sov. Phys.-Dokl. 7, 728 (1963)).

Krotikov, V. D. (1962). Some Electrical Properties of Earth Rock and Their Comparison with the Properties of the Surface Layer of the Moon. Izv. Vysshikh Uchebn. Zavedenii Radiofiz. 5, 1057.

Kuzmin, A. D. (1964). Concerning a Model of Venus with a "Cold" Absorbent Atmosphere. Izv. Vysshikh Uchebn. Zavedenii Radiofiz. 7, 1021.

Kuzmin, A. D. (1967). Radiophysics. 1965-1966. Radiophysical Investigations of Venus. In the series: Physics, All-Union Institute of Scientific and Technical Information, Academy of Sciences USSR, Moscow. (Eng. transl.: NASA Tech. Transl. F-536, Washington (1969)).

Lastochkin, V. P., Sorin Yu. M., and Stankevich, K. S. (1964). Spectrum of Radio Emission from Cygnus-A. Astron. Zh. 41, 770. (Eng. transl.: Sov. Astron.-AJ 8, 613 (1965)).

Law, S. E. and Staelin, D. H. (1968). Measurements of Venus and Jupiter near 1-cm Wavelength. Astrophys. J. 154, 1077.

Lazarevskii, V. S., Stankevich, K. S., and Troitskii, V. S. (1963). Precise Absolute Measurements of the Flux Density of the Crab and Orion Nebulae at 3.2 cm. Astron. Zh. 40, 12. (Eng. transl.: Sov. Astron.-AJ 7, 8 (1963)).

Lynn, V. L., Meeks, M. L., and Sohigian, M. D. (1964). Observations of Venus, the Region of Taurus A, and the Moon at 8.5-Millimeter Wavelength. Astron. J. 69, 65.

MacLeod, J. M. (1971). Private Communication.

Mayer, C. H., McCullough, T. P., and Sloanaker, R. M. (1958). Observations of Venus at 3.15-cm Wave Length. Astrophys. J. 127, 1.

McAdam, B. (1971). Private Communication.

Morrison, D. (1969a). Venus: Absence of a Phase Effect at a 2-Centimeter Wavelength. Science 163, 815.

Morrison, D. (1969b). Ph.D. Thesis, Harvard University.

Morrison, D. (1970). Thermophysics of the Planet Mercury. Space Sci. Rev. 11, 271.

Muhleman, D. O. (1961). Early Results of the 1961 JPL Venus Radar Experiment. Astron. J. 66, 292.

Muhleman, D. O. (1963). The Electrical Characteristics of the Atmosphere and Surface of Venus from Radar Observations. Icarus 1, 401.

Muhleman, D. O. (1969). Microwave Opacity of the Venus Atmosphere. Astron. J. 74, 57.

Pettengill, G. H., Briscoe, H. W., Evans, J. V., Gehrels, E., Hyde, G. M., Kraft, L. G., Price, R., and Smith, W. B. (1962). A Radar Investigation of Venus. Astron. J. 67, 181.

Pollack, J. B. and Morrison, D. (1970). Venus: Determination of Atmospheric Parameters from the Microwave Spectrum. Icarus 12, 376.

Scheuer, P. A. G. and Williams, P. J. S. (1968). Radio Spectra. Ann. Rev. Astron. and Astrophys. 6, 321.

Sinclair, A. C. E., Basart, J. P., Buhl, D., Gale, W. A., and Liwshitz, M. (1970). Preliminary Results of Interferometric Observations of Venus at 11.1-cm Wavelength. Radio Sci. 5, 347.

Stankevich, K. S. (1962). Precision Measurements of the Spectrum of the Discrete Source Cassiopeia-A in the Centimeter Region. Astron. Zh. 39, 610. (Eng. transl.: Sov. Astron.-AJ 6, 480 (1963)).

Stankevich, K. S. (1970). Observations of Mars and Venus at 11.1 cm. Australian J. Phys. 23, 111.

Strelkov, G. M. (1967). Emission and Reflectivity of Venus in the Decimeter Wavelength Range. Dokl. Akad. Nauk. SSSR 174, 1292. (Eng. transl.: Sov. Phys. - Dokl. 12, 532 (1967)).

Tikhonova, T. V. and Troitskii, V. S. (1969). Effect of Heat from within the Moon on its Radio Emission for the Case of Lunar Properties which Vary with Depth. Astron. Zh. 46, 159. (Eng. transl.: Sov. Astron.-AJ 13, 120 (1969)).

Vinogradov, A. P., Surkov, Yu. A., Andreichikov, B. M., Kalinkina, O. M., and Grechischeva, I. M. (1971). The Chemical Composition of the Atmosphere of Venus. In Planetary Atmospheres, I.A.U. Symposium No. 40 (Sagan, C., Owen, T. C., and Smith, H. J., eds.), D. Reidel Pub. Co., Dordrecht-Holland, p. 3.

VITA

William Wallace Warnock was born on April 23, 1944 in Monmouth, Illinois and reared in Alexis, Illinois. He attended Western Illinois University at Macomb from September, 1962 until June, 1964. After transferring to the University of Illinois at Urbana-Champaign in September, 1964, he obtained there the degree of Bachelor of Science in Electrical Engineering in February, 1967 and was named valedictorian of his graduating class. His graduate studies at the University of Illinois at Urbana-Champaign extended from February, 1967 to October, 1971.

During the summer of 1966 he was employed as a Junior Engineer by the Jet Propulsion Laboratory in Pasadena, California. He is a member of Eta Kappa Nu, Tau Beta Pi, Phi Kappa Phi, and the American Astronomical Society. He is a co-author, with J. R. Dickel and W. J. Medd, of "Lack of Phase Variation of Venus" in Nature 220, 1183 (1968).